

CHAOTIC SPREADING OF EPIDEMICS IN COMPLEX NETWORKS OF EXCITABLE UNITS

F.S. VANNUCCHI AND S. BOCCALETTI

Istituto Nazionale di Ottica Applicata
Largo E. Fermi, 6
50125 Florence, Italy

(Communicated by Ying-Cheng Lai)

ABSTRACT. We explore the dynamics of an epidemiological disease spreading within a complex network of individuals. The local behavior of the epidemics is modelled by means of an excitable dynamics, and the individuals are connected in the network through a weighted small-world wiring. The global behavior of the epidemics can have stationary as well as chaotic states, depending upon the probability of substituting short-range with long-range interactions. We describe the bifurcation scenario leading to such latter states, and discuss the relevance of the observed chaotic dynamics for the description of the spreading mechanisms of epidemics inside complex networks.

1. Introduction. During years, there has been an intense activity in the study of epidemic outbreaks and disease spreading in complex networks. In particular, attention has been centered inspecting networks sharing important topological features, such as the small-world (SW) properties [1] and the scale-free (SF) degree distribution [2], over which epidemiological models have been implemented [3, 4]. Many important results, such as the setting of a threshold for an epidemic outbreak depend crucially on the statistical properties of the underlying network connectivity distributions [5, 6].

Furthermore, it has been established that SW and SF properties well characterize the structure of interactions in real-world networks of both artificial and natural systems [5, 6, 7, 8, 9].

In this paper we study the dynamics of a spreading epidemiological disease in a complex network of excitable units, whose wiring geometry is properly constructed to model social connectivities between individuals, where short-range (nearest neighbors) and long-range interactions between nodes are taken into account.

2. The local dynamics. The system under study is a network made of 1000×1000 bi-dimensionally ordered sites. Each site (i, j) is associated with two dynamical variables, an activator variable $(u_{i,j})$ and an inhibitor variable $(v_{i,j})$, obeying the standard FitzHugh-Nagumo equations [10, 11]

$$\frac{\partial u_{i,j}}{\partial t} = -u_{i,j}(a - u_{i,j})(1 - u_{i,j}) - v_{i,j} + C_{i,j}, \quad (1)$$

2000 *Mathematics Subject Classification.* 92D30, 34D20.

Key words and phrases. Complex networks, excitable media, chaotic dynamics.

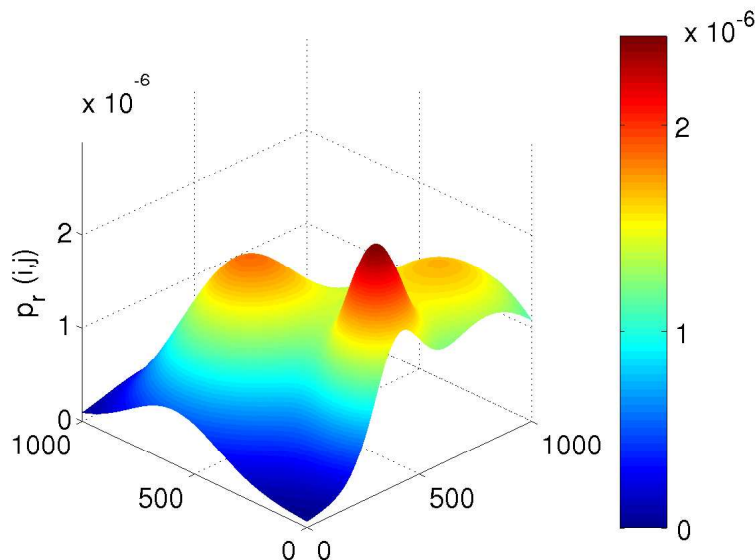


FIGURE 1. Three-dimensional graph of the receiving probability $p_r(i, j)$ (see text for definition). The values of p_r are normalized so $\sum_{i,j=1}^{1000} p_r(i, j) = 1$.

$$\frac{\partial v_{i,j}}{\partial t} = e * u_{i,j}. \quad (2)$$

Here, a is the excitability threshold, and e a suitable real parameter. Furthermore, $C_{i,j}$ represents the network coupling term acting on the (i, j) site, that will be specified in the following. When choosing $e = 0.0017$ and $a = 0.13$, the local dynamics is set within the excitable regime. In these conditions, and for $C(i, j) \equiv 0$, each network unit stays in its stable stationary state ($u_{i,j} = v_{i,j} = 0$), until a finite perturbation (of size exceeding a) in the variable u starts the evolution of an excitable pulse. During the pulse, the variable u grows until reaching the right stable branch of the null cline $-u_{i,j}(a - u_{i,j})(1 - u_{i,j}) - v_{i,j} = 0$, where an increase of the variable v starts. When v is sufficiently high, the variable u begins to decrease, and drops onto the left stable branch of the null cline $-u_{i,j}(a - u_{i,j})(1 - u_{i,j}) - v_{i,j} = 0$. Finally, the whole dynamics relaxes back to the initial stationary state.

It is well known that one can distinguish among different phases during the excitable dynamics [12]. Precisely, when the system is lying on the stationary state, we are in a quiescent state, where the system is available to start the dynamics if a proper perturbation is applied. In the following we will associate such a state to the susceptible state of individuals. A second phase can be distinguished in the totally refractory state, i.e. the state presented by the system for the whole period in time in which the dynamics develops onto the right stable branch of the null cline $-u_{i,j}(a - u_{i,j})(1 - u_{i,j}) - v_{i,j} = 0$. Here, the system is practically insensitive to perturbation of any size, and we will associate this state with the refractory period of individuals during the evolution of their disease (the fact that an infected individual cannot be further infected by the same disease). Finally, the recovery dynamics toward the stationary state can be associated with a relative refractory state, wherein another excitable pulse can be produced for perturbations larger

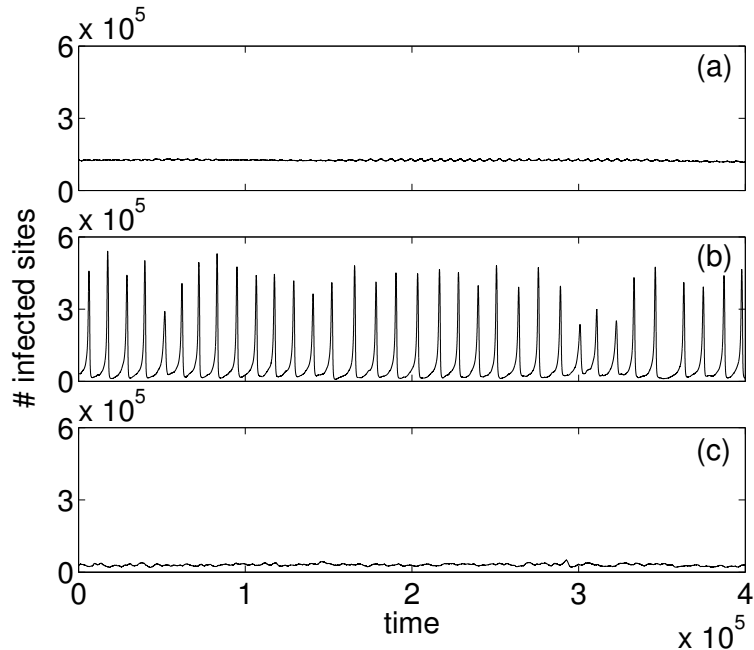


FIGURE 2. Temporal evolution of the total number of infected individuals N in the network for different values of the breaking probability P . (a) $P = 5\%$; (b) $P = 10\%$; (c) $P = 12\%$. All other parameters are specified in the text.

than the ones necessary in the stationary state. This relative refractory state well mimics the recovery of individuals from diseases, modelling the fact that a single individual recovering from a disease is somehow more robust (for a limited amount of time) against a second infection process of the same disease.

3. The connectivity network. In order to proceed, we now have to specify the network coupling term $C(i, j)$ in Eqs. (1,2). In doing this, we want to model a realistic social wiring connecting individuals susceptible of being infected by a given disease.

We start by connecting each site diffusively with its nearest neighbors, that implies $C(i, j) = D(u_{i+1,j} + u_{i-1,j} + u_{i,j+1} + u_{i,j-1} - 4u_{i,j})$, being D a diffusion coefficient (in what follows we set $D = 0.13$). This models the situation in which an infected individual ($u > a$) can transmit the disease only to its nearest neighbors individuals. In this condition, it is well known that an initial seed of excitation gives rise to a transient dynamics characterized by a target excitation pattern, moving toward the boundary of the two-dimensional system and eventually disappearing. As a result, the only asymptotic behavior that can be expected in this case is a situation where the epidemics disappears.

A more realistic description of social connections must account for the possibility of an infected individual to transmit the disease also to other individuals located far away from it, as it is the case of travelling individuals, that are moving between very far away points of the network. This feature is accounted for by assigning to

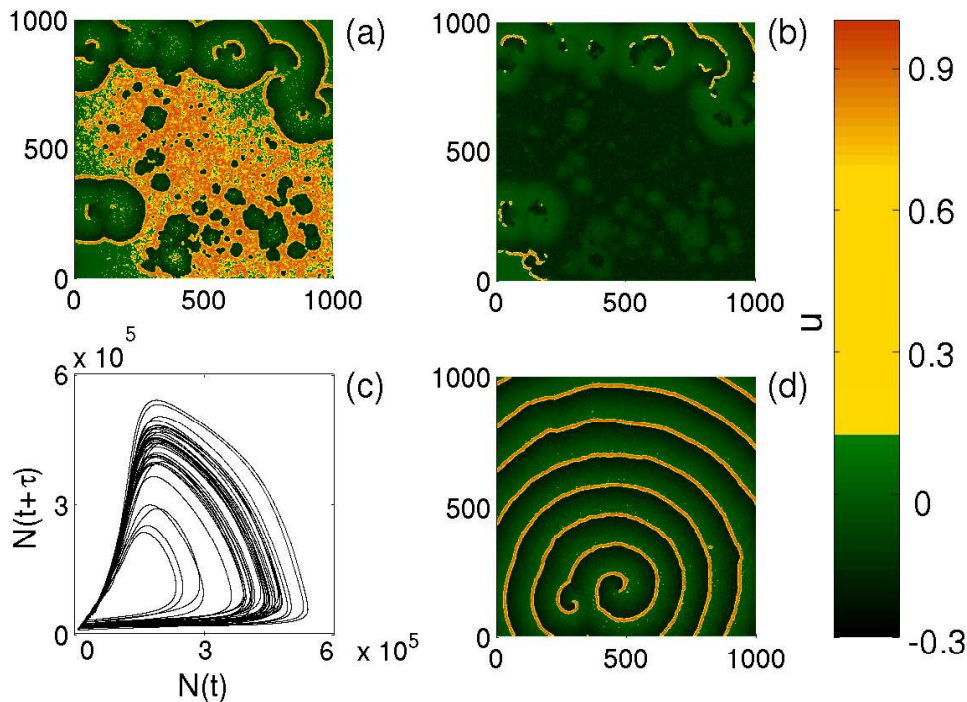


FIGURE 3. Upper row: Spatial pattern of the variable u for $P = 10\%$, corresponding to a maximum (a) and a minimum (b) of the oscillations reported in Fig. 2b. (c) Two-dimensional projection of the time-delay embedding reconstruction of the attractor corresponding to the dynamics of N for $P = 10\%$. The time evolution of the infected sites number (as it appears in Fig. 2b) is plotted against its value delayed of an embedding time $\tau = 71,7$ units of time. (d) Typical spatial pattern of the variable u for $P = 5\%$, characterizing the almost constant temporal behavior reported in Fig. 2a.

each one of the four original connections a probability $0 \leq P \leq 1$ of being substituted with a connection with any other site of the network, in the very same spirit of small-world wirings [1]. To make this long-range interaction process even more realistic, we have further elaborated the structure of our network by differentiating the *receiving probability* $p_r(i, j)$ of each site: when a local connection is broken, it is substituted by a connection with a network site extracted from the non-homogeneous probability distribution $p_r(i, j)$ reported in Fig. 1. This means that there are more probable destinations for each travelling individual within the network, as is the case for realistic social connections, where individuals travel preferably toward a limited number of target places. This is at variance with the original construction of small-world networks [1], where the probability $p_r(i, j)$ was homogeneously taken within the network.

With the above stipulations, we have performed a series of simulations of Eqs. (1,2) at different values of P . Simulations were performed by means of a Runge-Kutta integration scheme for the time evolution of the local dynamics, complemented by a "Crank-Nicholson" method [13] for the treatment of the diffusion term $C(i, j)$, with open boundary conditions. As for initial conditions, we have initiated a localized seed of infected individuals ($u > a$) given by a Gaussian distribution centered at the site $(i, j) = (200, 700)$ and with a standard deviation of 10 network sites (this initial condition corresponds to setting a total of 0.12% of sites in the infected state). The initial values of $v_{i, j}$ were taken at zero everywhere. After a transient time of approximately $2 * 10^6$ Runge-Kutta integration intervals, the whole dynamics entered the asymptotic regime and the corresponding results were monitored.

4. Results and discussion. Relevant information on the dynamics of our system can be gathered by monitoring the temporal evolution of the total number of infected individuals N at different values of P . An individual is marked as infected if the corresponding value of the u variable exceeds the excitability threshold $a = 0.13$.

The results are shown in Fig. 2. For $P = 0$, our network is a standard excitable media whose sites are diffusively connected. As we have already discussed above, an initial seed in these conditions gives rise to a target pattern of infected individuals, that affects the network only for a transient time, while asymptotically $N(t) = 0$. As P increases, the system begins to support a self-sustained asymptotic dynamics, leading initially to an almost constant value of $N(t)$ (see Fig. 2a, obtained for $p = 0.05$).

A further increase of P generates oscillations in the asymptotic dynamics of $N(t)$. For $0.09 < P < 0.11$, these oscillations become very large in size and chaotic. This is a remarkable result, since it resembles the common behavior of many real epidemiological diseases having an almost cyclic behavior, in which periods where the epidemics is almost totally removed alternates with other periods where very large peaks in the epidemics are measured. An example of such situation is shown in Fig. 2b, obtained for $P = 0.1$.

Finally, Fig. 2c shows the situation occurring at higher values of P where oscillations in $N(t)$ are removed and an almost constant behavior is again set in our network.

Other important information on the evolution of the spreading disease can be obtained by inspecting snapshots of the spatial distribution of u at different times. Precisely, Fig. 3a (3b) reports the spatial distribution of u inside the chaotic regime ($P = 10\%$) occurring in correspondence to a maximum (a minimum) of the oscillations reported in Fig. 2b. Here, one clearly sees that the spatial structure of the network shows coexistence of macroscopic domains of infected individuals with other macroscopic domains of non-infected sites. This feature again realistically models many situations where the epidemic outbreaks occur at a given time only in specific geographical regions, whereas other geographical regions at the same time appear to be unaffected by the disease. During the evolution of the system we furthermore observe motion of the domain walls between infected and non infected domains, as well as nucleation processes of diseases within domains of non infected (susceptible) individuals.

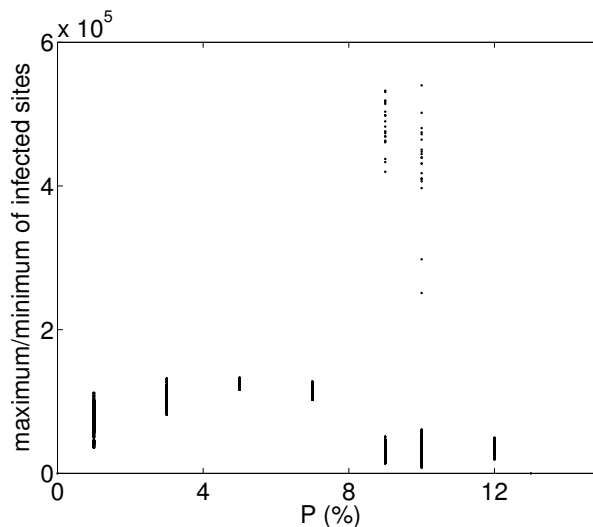


FIGURE 4. Bifurcation diagram of the observed network dynamics. At each value of P (horizontal axis, in percent) all values of local maxima and minima in the dynamics of the number N of infected sites in the corresponding time series are reported in the vertical axis.

In Fig. 3c we report the two-dimensional projection of the time-delay embedding reconstruction of the attractor corresponding to the dynamics of N for $P = 10\%$ (to be compared with Fig. 2b). In doing so, the time evolution of N is plotted against its value delayed of an embedding time $\tau = 71,7$ units of time, highlighting the chaotic nature of the dynamics. An exhaustive characterization of the chaotic regime, including evaluation of Lyapunov exponents for the dynamics of N and a detailed analysis of the corresponding domain motion and interactions, will be reported elsewhere.

For comparison, Fig. 3d shows a typical spatial distribution of the variable u for $P = 0.05$, characterizing the almost constant temporal behavior of $N(t)$ reported in Fig. 2a, and resembling the complex patterns that have been largely observed and characterized in various standard excitable media in the presence of purely diffusive coupling (such as in the case of ventricular fibrillation of a two dimensional cardiac tissue [14] or in Belousov-Zhabotinski chemical reactions [15]).

Finally, in Fig. 4 we show the bifurcation scenario of the observed network dynamics. Precisely, at each value of P (reported in percent on the horizontal axis) the different values of local maxima and minima in the corresponding time series of $N(t)$ are reported, showing the transition from an almost constant behavior ($P < 0.09$) to chaotic oscillations ($0.09 \leq P \leq 0.11$) to again an almost constant evolution ($P \geq 0.11$).

In conclusion, we have reported the dynamics of a complex network of individuals subjected to a developing epidemiological disease. The process of infection-recovery from the disease has been modelled by means of an excitable dynamics, and the connection between individuals has been accounted for by a weighted small-world wiring. Our results indicate that the global behavior of the epidemics can have stationary as well as chaotic states, depending upon the probability of substituting

short-range with long-range interactions. Furthermore, the chaotic regime is characterized by a spatial evolution of the epidemics wherein macroscopic domains of infected and susceptible sites coexist and interact. We argue that many of these features indeed resemble what is observed in realistic social networks during the spreading mechanism of epidemiological diseases.

Acknowledgments. The Authors are indebted with Y. Moreno and K. Showalter for many fruitful discussions on the subject. Work partly supported by EU Contract HPRN-CT-2000-00158, and MIUR-FIRB project n. RBNE01CW3M-001.

REFERENCES

- [1] D.J. Watts and S.H. Strogatz, *Nature* **393**, 440 (1998).
- [2] A.-L. Barabási and R. Albert, *Science* **286**, 509 (1999).
- [3] R. Pastor-Satorras and A. Vespignani, *Phys. Rev. Lett.* **86**, 3200 (2001).
- [4] A.L. Lloyd and R.M. May, *Science* **292**, 1316 (2001).
- [5] D.J. Watts, *Small worlds: the dynamics of networks between order and randomness* (Princeton University Press, New Jersey, 1999).
- [6] A.-L. Barabási and R. Albert, *Rev. Mod. Phys.* **74**, 42 (2002).
- [7] R. Albert, H. Jeong and A.-L. Barabási, *Nature* **401**, 130 (1999).
- [8] S.H. Strogatz, *Nature* **410**, 268 (2001).
- [9] J. M. Montoya and R.V. Solé, *J. Theor. Biol.* **214**, 405 (2002).
- [10] R. FitzHugh, *Biophys. J.* **1**, 445 (1961).
- [11] J. Nagumo, S. Arimoto and S. Yoshizawa, *Proc. I.R.E.* **50**, 2061 (1962).
- [12] For a comprehensive review on pattern formation and competition in excitable media see E. Meron, *Phys. Rep.* **218**, 1 (1992), and References therein.
- [13] W. Press, S. Teukolsky, W. Vetterling and B. Flannery, *Numerical Recipes in C: The Art of Scientific Computing*, chapters XVI and XIX.
- [14] D.R. Chialvo and J. Jalife, *Nature* **330**, 749 (1987).
- [15] M. Markus and B. Hess, *Nature* **347**, 6288 (1990).

Received on Feb. 1, 2004. Revised on Feb. 16, 2004.

E-mail address: `fabio@ino.it`

E-mail address: `stefano@ino.it`